Measurements of the absolute photoionization cross section of Fe^+ ions from 15.8 to 180 eV

2002 J. Phys. B: At. Mol. Opt. Phys. 35 3655

(http://iopscience.iop.org/0953-4075/35/17/303)

INSTITUTE OF PHYSICS PUBLISHING JOURNAL OF PHYSICS B: ATOMIC, MOLECULAR AND OPTICAL PHYSICS

J. Phys. B: At. Mol. Opt. Phys. **35** (2002) 3655–3668 PII: S0953-4075(02)37259-6

Measurements of the absolute photoionization cross section of Fe^+ ions from 15.8 to 180 eV

H Kjeldsen, B Kristensen, F Folkmann and T Andersen

Institute of Physics and Astronomy, University of Aarhus, DK-8000 Aarhus C, Denmark

E-mail: kjeldsen@ifa.au.dk

Received 3 May 2002
Published 20 August 2002
Online at stacks.iop.org/JPhysB/35/3655

Abstract

The absolute single- and double-photoionization cross sections of singly charged Fe ions have been measured from 15.8 to 180 eV using the merged-beam technique. The data yield information about the photoionization continua and the resonance structures resulting from excitation of the outer 3d and 4s electrons as well as the inner 3p and 3s electrons. The vast majority of the Fe^+ target ions were present in the ground-state configuration, $3d^64s$, and term, ^6D. The experimental data have been compared with several calculations, for example *R*-matrix calculations from the Opacity Project and data obtained using the central-field approximations. The experimental data are available at http://www.ifa.au.dk/amo/atomphys/atomphys.htm.

1. Introduction

Absolute cross sections for photoionization of atoms and ions are essential data for the understanding of fundamental atomic physics, and in addition these cross sections are required for the modelling of numerous physical systems, for example astrophysical and terrestrial plasmas. The astrophysical requirements have been the main motivation for the extensive theoretical work performed either by individual groups or as part of one of several international collaborations. Among the latter, the Opacity Project (Seaton 1987, The Opacity Project Team 1995) deserves special attention: its goal was to calculate the photoionization cross sections for a large number of relatively light atoms and ions of astrophysical relevance using a sophisticated but effective approach based on the close-coupling approximation in combination with the *R*-matrix method. Thus, the quantity of calculated data available is very large. However, the calculations have generally not been tested by experimental absolute cross sections, because the data required only exist for relatively few cases (see below).

Neutral Fe and its ions play important roles in many aspects of astrophysics. Fe^+ has a relatively high cosmic abundance due to the significant abundance of the Fe element and the low ionization potential of neutral iron, 7.90 eV (NIST 2002), i.e. below the Lyman edge.

Furthermore, the Fe^+ spectrum is very rich on lines. The consequence is that this species forms the most common spectrum in astrophysics (Li *et al* 2000).

Also, iron occupies a special position (together with other transition elements) within fundamental atomic physics as its behaviour is interesting but difficult to describe; a comprehensive review about photoionization of metal atoms has been published by Sonntag and Zimmermann (1992). The large number of possible terms resulting from the approximately half-open 3d shell in combination with the near degeneracy of the $3d^x$, $3d^{x-1}4s$, $3d^{x-2}4s^2$ and other configurations for the neutral elements and the low-charged ions result in very complex systems, strongly influenced by configuration interaction. The situation is further complicated when the so-called 'giant resonance' resulting from excitation of the inner 3p electrons, i.e. the region of the $3p \rightarrow 3d$ transitions, is considered, because additional strong interactions occur between configurations of the $3p^5 3d^x nl$ and $3p^6 3d^{x-1} \epsilon l$ types. Therefore, calculations become extremely cumbersome and the spectra very rich on structure and difficult to analyse. The complications in the theoretical description may be matched by the experimental difficulties in producing and handling iron atoms and ions. These arise from the high temperature required for the vaporization of iron, the reactive nature of the metal vapour, the possible presence of several metastable states and the line-richness of the spectra observed.

Due to the general interest—and in spite of the difficulties present—a large number of theoretical and experimental investigations have been performed with the purpose of obtaining data concerning the atomic structure and processes involving iron atoms and ions. If we concentrate on studies related to Fe^+ ions and only give a few examples, we might mention Sugar and Corliss (1985) for energy levels, Nahar (1996, 1997) for $Fe^{2+} + e$ and $Fe^+ + e$ recombination rates, Li *et al* (2000) and Rostobar *et al* (2001) for lifetimes and transition probabilities, and Reilman and Manson (1978), Verner *et al* (1996), Nahar and Pradhan (1994) and Berrington and Ballance (2001) for photoionization cross sections, together with the references given in the quoted papers.

Only relatively few photoionization/photoabsorption experiments have been performed with iron atoms and ions. The essential investigations of emission lines, which have been observed and used to establish the positions of many of the low-lying energy levels for most iron ions, were mentioned above; see Sugar and Corliss (1985) and references therein or NIST (2002). For neutral iron, photoionization cross section measurements have been performed for the threshold region (Lombardi *et al* 1978, Hansen *et al* 1977) as well as for the region of the $3p \rightarrow 3d$ transitions (Feist *et al* 1996). However, the absolute photoionization cross section has only been measured at a single energy: Lombardi *et al* reported the cross section to be $(5.0^{+0.4}_{-0.7}) \times 10^{-18}$ cm^2 at 8.05 eV. The situation is even less satisfactory for the ions of Fe, since no experimental photoionization cross sections (relative or absolute) to our knowledge have been reported so far, in spite of the importance of such data.

Several *ab initio* calculations of the cross section for photoionization of Fe^+ ions have been performed and in some cases with very different results. As part of the Opacity Project, Sawey and Berrington (1992) calculated the cross section for photoionization of Fe^+–Fe^{3+} in the respective threshold regions utilizing the close-coupling approximation in combination with the *R*-matrix method. In the case of Fe^+, they employed a basis set consisting of 16 *LS* terms for the description of the target states, i.e. the configurations of the Fe^{2+} core, and they obtained a cross section which did not exhibit any sharp resonance structures. Later, Nahar and Pradhan ((1994), also as part of the Opacity Project) performed a more comprehensive calculation using the same technique but this time including 83 *LS* terms to describe the Fe^{2+} target states. In contrast to Sawey and Berrington, Nahar and Pradhan observed a very rich structure in the threshold region, 16–26 eV. In both cases, the calculations were performed in a non-relativistic approximation. To our knowledge, there exists only one *ab initio* calculation that considers

photoionization of the 3p inner-shell electrons of Fe^+ ions in some detail (but several for neutral Fe). The Fe^+ investigation was performed recently by Berrington and Ballance (2001). The *R*-matrix method was applied, but this time using an improved version which allowed inner-shell processes to be investigated; the basis set included 198 configurations to describe the Fe^{2+} target states. The main goal for Berrington and Ballance was to develop a technique suitable for calculating double-ionization cross sections for complex systems, such as Fe and Fe^+, yet they also provided the single-ionization cross section. Finally, Reilman and Manson (1978) and Verner *et al* ((1996), and references therein) have performed Hartree–Fock–Slater and Hartree–Dirac–Slater calculations, respectively, of the continuum cross sections.

For all the calculations mentioned above, the problem remains that experimental photoionization cross sections are not available to compare with, and thus their accuracies are unknown. The problem is especially severe considering the complexity of the Fe^+ ion. The lack of an experimental cross section reflects the experimental difficulties related to producing and characterizing a dense target of Fe^+ ions. However, absolute photoionization cross sections can in principle be measured utilizing the so-called merged-beam technique (characterized by collinearly overlapping beams of ions and photons) as first demonstrated by Lyon *et al* (1986) for Ba^+ ions. With the construction of undulator beam-lines at synchrotron-radiation facilities and the resulting availability of intense beams of VUV photons, it has become possible to measure even relatively small photoionization cross sections with high accuracy using this technique. So far, absolute cross sections obtained have been reported for positive ions of C (Kjeldsen *et al* 1999a, 2001, Müller *et al* 2002), N (Kjeldsen *et al* 2002a), O (Kjeldsen *et al* 2002a, Covington *et al* 2001), Mg (Kjeldsen *et al* 2000, West *et al* 2001), Al (West *et al* 2001), S (Kristensen *et al* 2002), and several heavier ions (see West (2001), Kjeldsen *et al* (2002b), and references therein).

In the present paper we report on the extension of this work to include the transition elements. At the University of Aarhus, Denmark, absolute cross-section data for photoionization of Fe^+ ions have been measured in the photon-energy range 15.8–180 eV, a region that is very relevant for astrophysical applications. The data cover the structure in the line-rich threshold region, the region of the $3p \rightarrow 3d$ resonances and the single- and double-ionization continua of the entire region.

2. Experimental procedure

The absolute photoionization cross-section data were measured at a merged-beam facility at the storage ring ASTRID. The experimental technique used to record the data presented here has already been described before, see e.g. Kjeldsen *et al* (1999b, 2001). In brief, the photoionization cross sections were obtained by merging the intense photon beam from the ASTRID undulator with a 2 keV beam of singly charged Fe^+ ions and measuring the resulting photoionization yield of doubly- and triply-charged ions. In addition, the current and velocity of the ion beam, the absolute photon flux (obtained using a photodiode), the magnitudes and overlaps of the two beams and the efficiency of the particle detectors used to record the photoionization yield (calibrated *in situ*) were determined and used to establish the *absolute* magnitudes of the photoionization cross sections. The photodiode was calibrated *in situ* utilizing a noble-gas ionization chamber with Ne. The photon-energy resolution in the experiments described here was 5–10 meV in the entire threshold region, ∼50 meV at 55 eV and increasing to ∼150 meV at 75 eV.

In general, the systematic uncertainty of the magnitude of the absolute photoionization cross sections measured with the present set-up has been 10–15%. However, in the present case the experimental data are influenced by the presence of higher-order radiation in the photon

beam and metastable ions in the target-ion beam, and it is important to clarify the effect of these 'contaminations'. The presence of higher-order radiation has the effect that the measured cross sections, σ_m, differ from the correct one, σ_0, in the following way: $\sigma_m = \sigma_0 \times A + B$ where the parameters A and B change relatively slowly with the photon energy, and $A \leqslant 1$ and $B \geqslant 0$ Mb. The fraction of higher-order radiation is generally only a problem for low photon energies, and thus $A \approx 1$ and $B \approx 0$ for photon energies larger that ∼25 eV. The effect of the metastable ions on the measured cross-section data depends (apart from the fraction of metastable ions) on the cross section of ions in their metastable state, compared to that of ground-state ions, and is therefore generally not possible to determine directly. The only exceptions are the cases where the spectra of the ground-state ions and the metastable ions can be separated, as was done for O^+ by Kjeldsen *et al* (2002a) and for Ca^+ by Kjeldsen *et al* (2002c), and those for which one of the spectra is already known. In the present investigation, the $^{56}Fe^+$ ions were produced in a hot-filament plasma ion source (Almen and Nielsen 1957) from volatile components resulting from the reaction of Fe grains and CCl_4. This technique has been observed to result in relatively cold ion beams, and thus the resulting beam consisted mainly of ground-state ions, but in addition it also contained a smaller fraction of metastable ions, probably ∼10% as discussed below. It has not been possible to determine the quantitative effect on the cross-section data from these metastable ions. However, for photon energies larger than 25 eV we expect that the cross section of ions in low-lying metastable states is almost equal to that of ground-state ions, and therefore we estimate that the systematic uncertainty of the present data with respect to the cross section of ground-state Fe^+ ions is less than 15%.

3. Results

The photoionization cross section of Fe^+ ions was measured from 15.8–180 eV and the entire data set is shown in figure 1. The ground state of Fe^+, $3s^2 3p^6 3d^6 4s\ ^6D_{J=9/2,7/2,...,1/2}$, is the dominant (>85%) component of the target-ion beam, but metastable states are expected to be present, mainly in the form of $3s^2 3p^6 3d^7\ ^4F_{J=9/2,7/2,...,3/2}$ ions; see below for further details. The total cross section exhibits intense resonances below 26 eV and in the region of 50–80 eV but is otherwise relatively flat, with a magnitude of the order 5 Mb below 120 eV decreasing to 2 Mb at 180 eV. The resonances at low photon energies are large in number, relatively intense, narrow and Lorentz-like. They arise from the excitation of the 3d valence electrons to autoionizing states of Fe^+. Excitation of electrons from the 3p inner shell is responsible for the broad, intense and asymmetric structure in the region of 50–80 eV (mainly the 3p → 3d transitions) and for the $Fe^+ \rightarrow Fe^{3+}$ double ionization (mainly 3p →ϵd photoionization followed by Auger decay).

3.1. The spectral structure in the threshold region and the beam composition

Figure 2 shows the region of the resonance(s) in the spectrum at 16.1–16.5 eV. The figure contains the experimental data and the data calculated by Nahar and Pradhan (1994). The discrepancies concerning splitting, intensity and background are evident and will be discussed below. The observed multiplet has been assigned to the $3d^6(^5D)4s\ ^6D_{J=9/2,7/2,...,1/2} \rightarrow 3d^5(^6S)4s(^7S)np\ ^6P_{J=7/2,5/2,3/2}$ transitions with $n = 5$ on the basis of a quantum-defect analysis. The fine-structure splitting is much smaller for the final state than for the initial state (∼5 meV compared to ∼50 meV for the $n = 4$ configuration (NIST 2002)), and consequently the splitting of the multiplet is essentially identical to the fine-structure splitting of the initial state.

The calculation by Nahar and Pradhan was carried out in the close-coupling approximation using the R-matrix method and a target state expansion consisting of 83 LS terms of Fe^{2+};

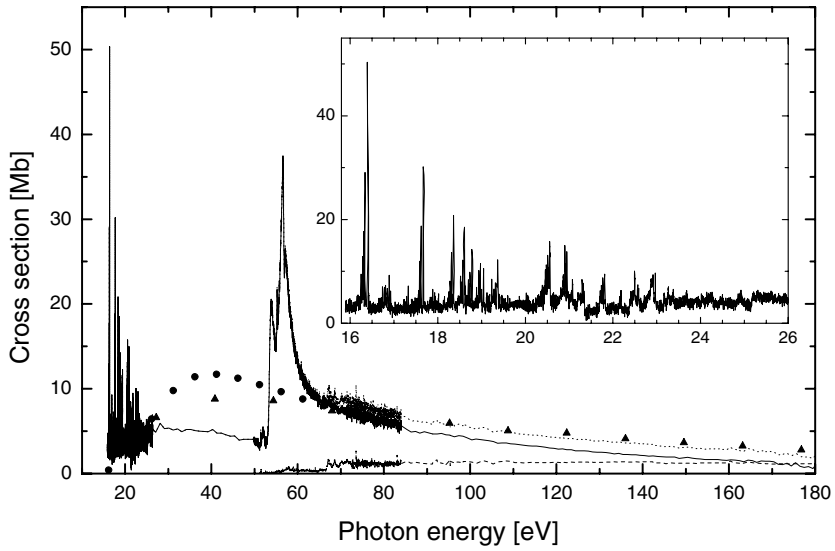

Figure 1. The measured absolute cross-section data for single (solid curve) and double (dashed curve) photoionization of Fe^+ together with their sum (dotted curve) in the photon-energy region 15.8–180 eV with details of the threshold region shown in the inset. The data below 25 eV are influenced by higher-order radiation, see text. Furthermore, the figure displays calculated data by Reilman and Manson (1978, triangles) and Verner *et al* (1996, circles).

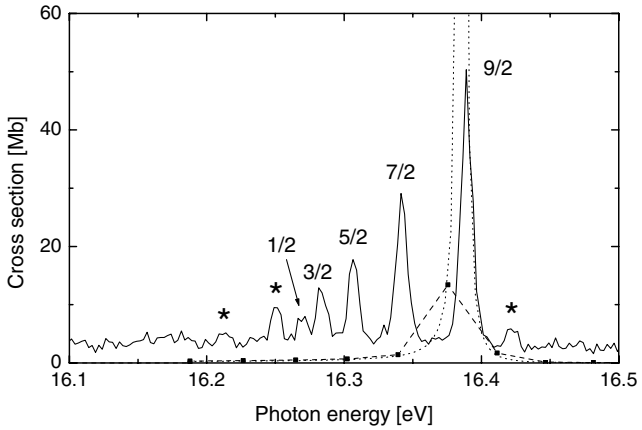

Figure 2. The photoionization cross section of Fe^+ ions in the 16.1–16.5 eV region containing the energetically lowest lying resonances in the spectrum. Experimental data: solid curve; calculated data: dashed curve and squares (Nahar and Pradhan (1994), original published data) and dotted curve (Nahar and Pradhan (1994), recalculated with a finer energy mesh). The calculated data have been shifted slightly according to the observed ionization threshold (NIST 2002). The initial J values belonging to the different $3d^6(^5D)4s^6\ D_{J=9/2,7/2,...,1/2} \rightarrow 3d^5(^6S)4s(^7S)\ 5p\ ^6P_{J=3/2,5/2,7/2}$ resonances are indicated, and the peaks, expected to result from photoionization of metastable Fe^+ ions, are marked by asterisks. The experimental data are influenced by higher-order radiation in this region, see text.

it is probably the most accurate *ab initio* calculation for the threshold region of Fe^+ reported so far. The calculation was performed in a non-relativistic approximation and therefore does not describe the spin–orbit splitting of the multiplet as observed in the experimental data. In

connection with the present work, Nahar and Pradhan repeated their calculation with exactly the same technique and basis set but a finer energy grid (Nahar 2002). The new calculation is shown together with the original one in figure 2. Evidently, the original energy grid is too coarse and results in apparently incorrect predictions of the position, intensity, shape and width of the resonance lines. The same problem has previously been observed for several other calculations, and therefore it should be stressed that it is an essential part of a photoionization cross-section calculation to ensure that the employed energy grid is sufficiently fine.

The additional (weak) lines in figure 2, marked by *, that cannot be assigned to the above-mentioned multiplet are assumed to arise from the metastable ions present in the target beam. The $3d^6(^5D)4s\ ^6D_{J=9/2,7/2,\ldots,1/2}$ ground-state levels constitute the dominating component of the target beam, and we can use the relative intensities of the five main peaks to estimate the ion-source temperature, if we assume that the oscillator strengths for the $3d^6(^5D)4s\ ^6D_{J_i} \rightarrow 3d^5(^6S)4s\ (^7S)np\ ^6P_{J_f}$ transitions are independent of the initial and final J values. Fitting $f_{J_i} \propto (2J_i + 1) \cdot \exp\frac{-E_i}{kT}$ (with E_i being the energy of the initial state) yields $kT \approx 0.12$ eV, a quite low value that should be compared with the energies of the metastable states, the first one being the $3s^23p^63d^7\ ^4F_{J=9/2,7/2,5/2,3/2}$ levels located at 0.232, 0.301, 0.352 and 0.387 eV, respectively, followed by the $3d^6(^5D)4s\ ^4D_{J=7/2,5/2,3/2,1/2}$ levels at $\sim$1 eV. Although the model may not be entirely correct it indicates that the ground-state J-levels are the dominating component of the target beam, constituting about 90%, followed by the $3s^23p^63d^7\ ^4F_J$ metastable states as the main contamination; the 90% is obtained using the above model with $kT = 0.12$ eV and comparing the population of all the low-lying Fe^+ states. In support of this assumption we notice that the main peaks can be assigned to transitions from the ground-state levels and that no peaks have been observed below 16.2 eV.

As mentioned above, the measured cross-section data below $\sim$25 eV can be significantly influenced by higher-order radiation. For the energy-region shown in figure 2 (and 3) the effect is that the measured peak intensities (i.e. the measured f values) are too small while the background (i.e. continuum) cross section is too large. This may account for the discrepancy with respect to the calculated data concerning the continuum cross section.

In order to compare the oscillator strengths of the resonances as obtained by the non-relativistic calculations by Nahar and Pradhan (1994) and by the experimental data, we need to utilize the sum of the measured oscillator strengths for the $3d^6(^5D)4s\ ^6D_{J=9/2,7/2,\ldots,1/2} \rightarrow 3d^5(^6S)4s(^7S)5p\ ^6P_{J=7/2,5/2,3/2}$ multiplet. It is observed that the calculated value (obtained using the fine-grid data) is about 50% larger than the sum of the experimental ones, a discrepancy which, at least partly, can be attributed to experimental problems concerning higher-order radiation or metastable target ions.

The entire threshold region is shown in figure 3. The region contains a large number of resonances from several Rydberg series of the type $3d^6(^5D)4s\ ^6D_{J_i} \rightarrow Fe^{2+}(^{2S+1}L)np$ or $nf\ ^{2S'+1}L'_{J_f}$. Considering one-electron transitions only and assuming LS coupling to be valid, the number of allowed Rydberg series is 23; these are listed in table 1. In addition, the fine-structure splitting of the initial and final states should be taken into account, two-electron transitions may be present and LS coupling can probably not be expected to be valid for high n values, all of this resulting in a complicated spectrum with a very large number of peaks. The assignment of the resonance lines is further complicated by the uncertainty of the experimental data due to statistical fluctuation, finite instrumental resolution, the presence of higher-order radiation and the possible population of metastable states.

With such a large number of partly overlapping series, it might appear less likely to perform a reliable assignment using quantum-defect theory, but in the case of the five lowest-lying Rydberg series (see table 1) the situation is simplified for the following reasons. Firstly, each Fe^{2+} state results only in two series of Rydberg states which can be accessed from the ground

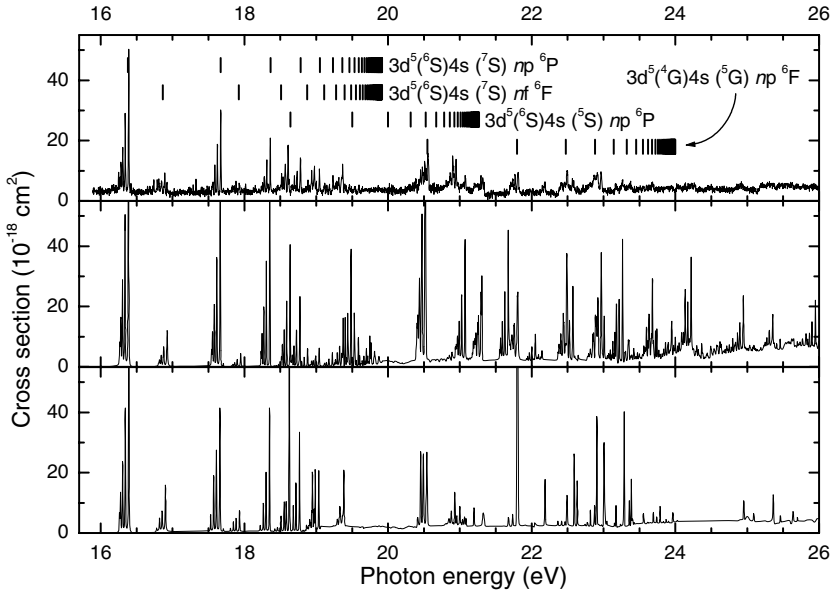

Figure 3. The entire threshold energy region. Top: present experimental data; middle: simulation using the calculation by Nahar and Pradhan (1994), recalculated with a finer energy mesh); bottom: relativistic *R*-matrix calculation by Berrington (2002a). Four different Rydberg series are indicated. The experimental data are influenced by higher-order radiation in this region, see text.

state, an *n*f and an *n*p series, but these are *not* further split into different terms. Secondly, the Fe^{2+} states (i.e. the series limits) are separated sufficiently to ensure relatively little overlap between the members of the different series, and therefore the effects of configuration interaction can be expected to be limited. Thirdly, the energy splittings of the Fe^{2+} cores due to relativistic effects are small for the relevant configurations. Furthermore, it is useful to notice that the *n*f series are expected to be much weaker and to have higher energies than the *n*p series due to the large centrifugal repulsion present in the effective potential for the f electron. Thus, it has been possible to identify the members of four out of the five first Rydberg series listed in table 1, and the assignments are indicated in figure 3. We notice that the strongest resonances are those closest to the Fe^+ ionization threshold, and that these belong to the first series listed in table 1, the $3d^6(^5D)4s\ ^6D_{J=9/2,7/2,...,1/2} \rightarrow 3d^5(^6S)4s(^7S)np\ ^6P_{J=7/2,5/2,3/2}$ transitions.

Apart from the experimental data, figure 3 also shows the calculation by Nahar and Pradhan (1994) for comparison. A direct comparison between the two data sets is hampered by the finite instrumental resolution and the fact that the calculation is performed in a non-relativistic approximation. Therefore an experimental spectrum has been compared with a simulated cross section, σ_{sim}, which was obtained utilizing the calculated data in the following way:

$$\sigma_{sim}(h\nu) = \sum_J \{P_J \cdot \sigma_J(h\nu)\} \otimes \text{instr.} \tag{1}$$

Here the P_J factors and $\sigma_J(h\nu)$ are the relative populations and cross sections, respectively, of the different $3d^6(^5D)4s\ ^6D_{J=9/2,7/2,...,1/2}$ states, and the last part of the equation represents the convolution with the instrumental function, approximated by a 7 meV (FWHM) Gaussian. The magnitude of the P_J factors was determined using the relative intensities of different transitions in the $3d^6(^5D)4s\ ^6D_{J=9/2,7/2,...,1/2} \rightarrow 3d^5(^6S)4s(^7S)5p\ ^6P_{J=3/2,5/2,7/2}$ multiplet as observed in the experimental spectrum in figure 2 in such a way that $\Sigma P_J = 1$. Since the calculation is

Table 1. The Rydberg series of one-electron transitions that are allowed within LS coupling and the series limits. Only transitions from the ground states, $3d^6(^5D)4s\,^6D_{J_i}$ are considered. (ID) indicates that members of a given series have been identified in the experimental data.

Rydberg series	Series limit (eV)
$3d^5(^6S)4s(^7S)$ { np ^6P_J (ID); nf ^6F_J (ID)	about 19.9
$3d^5(^6S)4s(^5S)$ { np ^6P_J (ID); nf ^6F_J	about 21.3
$3d^5(^4G)4s(^5G)$ { np ^6F_J (ID); nf { ^6P_J, ^6D_J, ^6F_J }	about 24.0
$3d^5(^4P)4s(^5P)$ { np { ^6P_J, ^6D_J }; nf { ^6D_J, ^6F_J }	about 24.4
$3d^5(^4D)4s(^5D)$ { np { ^6P_J, ^6D_J, ^6F_J }; nf { ^6P_J, ^6D_J, ^6F_J }	about 24.8
$3d^5(^4F)4s(^5F)$ { np { ^6D_J, ^6F_J }; nf { ^6P_J, ^6D_J, ^6F_J }	about 26.5

non-relativistic $\sigma_J(h\nu) = \sigma(h\nu - \Delta E_J)$, with ΔE_J being the energy of the Fe^+ ground-state fine-structure levels compared to the $J = \frac{9}{2}$ level and $\sigma(h\nu)$ the cross section calculated by Nahar and Pradhan (fine-grid version). Thus, we assume that the spectra for the different spin–orbit component of the ground state are identical, except for an energy shift. It would also have been possible to include metastable states in the simulation, but doing this did not improve the agreement between theory and experiment and the idea was therefore abandoned.

It can be observed from figure 3 that the calculation has predicted the energies and intensities of the peaks in the 16–20 eV region rather accurately. For higher energies, 20–26 eV, there exist discrepancies between the experimental and the calculated data concerning the spectral structure, especially with respect to the intensities of the resonances, but also the magnitude of the calculated continuum cross section in the 26–30 eV region (not shown), which is much larger than the experimental value (for example 9 Mb compared to 5 Mb at 30 eV).

Recently, Berrington (2002a, 2002b) has performed relativistic R-matrix calculations of the photoionization cross section of Fe^+ in the threshold region. The final states, in particular, have been improved in comparison with those of Nahar and Pradhan (1994). Like Nahar and Pradhan, Berrington also employed an energy grid that was too coarse, and data using a finer grid have only been obtained for the 16–17 eV region; the calculated spectrum is also shown in figure 3. The agreement with the experimental data is comparable to the case for the

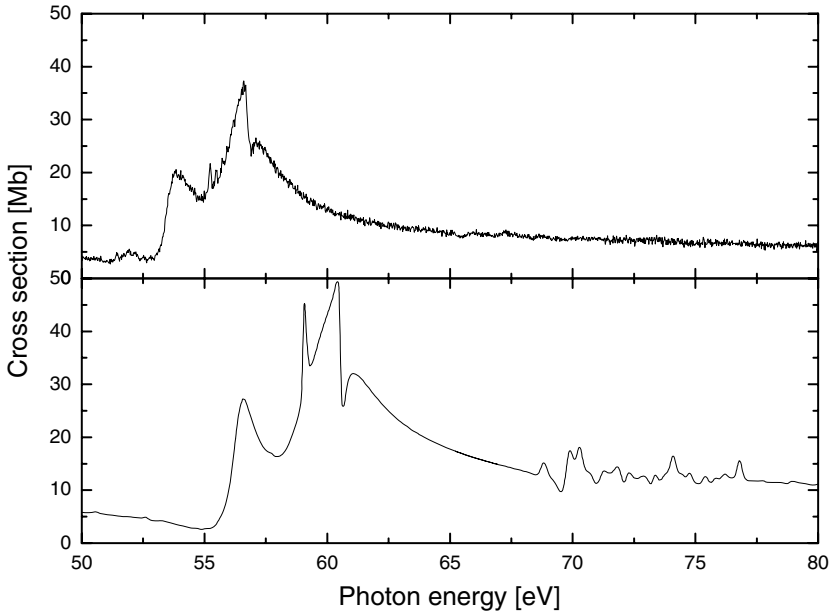

Figure 4. The $Fe^+ \rightarrow Fe^{2+}$ single-photoionization cross section in the region of the $3p \rightarrow 3d$ transitions. The figure presents the experimental data (top) and the data calculated by Berrington and Ballance ((2001) bottom); the calculated data have been convoluted with a Gaussian, representing the experimental resolution (FWHM = 50 meV for $h\nu \leqslant 65$ eV and 200 meV for $h\nu > 65$ eV).

calculation by Nahar and Pradhan, yet the calculated oscillator strength of the resonances lines near 16.3 eV (their sum) is about 25% smaller and thus closer to the experimental value and the agreement concerning the continuum cross section in the 26–30 eV region is also very good. For both calculations, good agreement is observed for the 16–17 eV region, except for an offset in the experimental cross section (∼3 Mb, due to higher-order radiation) and a scaling factor of ∼50% (Nahar and Pradhan 1994) or ∼65% (Berrington 2002a) respectively; the scaling factors are probably partly due to the presence of higher-order radiation and metastable ions.

Finally, it should be mentioned that new relativistic *R*-matrix calculations are in progress at the Ohio State University (Pradhan 2002).

3.2. The region of the 3p → 3d transitions

Figures 4 and 5 show the single- and double-photoionization cross sections, respectively, of Fe^+ ions in the region of the $3p^{-1}$ ionization thresholds. The single-ionization cross section (figure 4) exhibits several peaks, some of them being broad and intense while other are narrow and weaker. The broad peaks are due to the $3p \rightarrow 3d$ transitions and appear to be almost Fano-like, whereas we expect the narrow ones to be due to $3p \rightarrow 4s$ transitions (Martins 2001). Due to the many coupling possibilities resulting from the open d shell and the near degeneracy of the $(\cdots)3d^x$, $(\cdots)3d^{x-1}4s$ and $(\cdots)3d^{x-2}4s^2$ configurations, there may exist several such transitions.

The large overlap between the 3p and 3d wavefunctions implies that the $3p \rightarrow 3d$ transitions are much more intense that the transitions from 3p to other d orbitals. However, it also has the consequence that the $3p^5 3d^7 4s$ states interact strongly with the $3p^6 3d^5 4s\epsilon l$ continua, implying a short lifetime of the former. In combination with the many coupling possibilities, the result

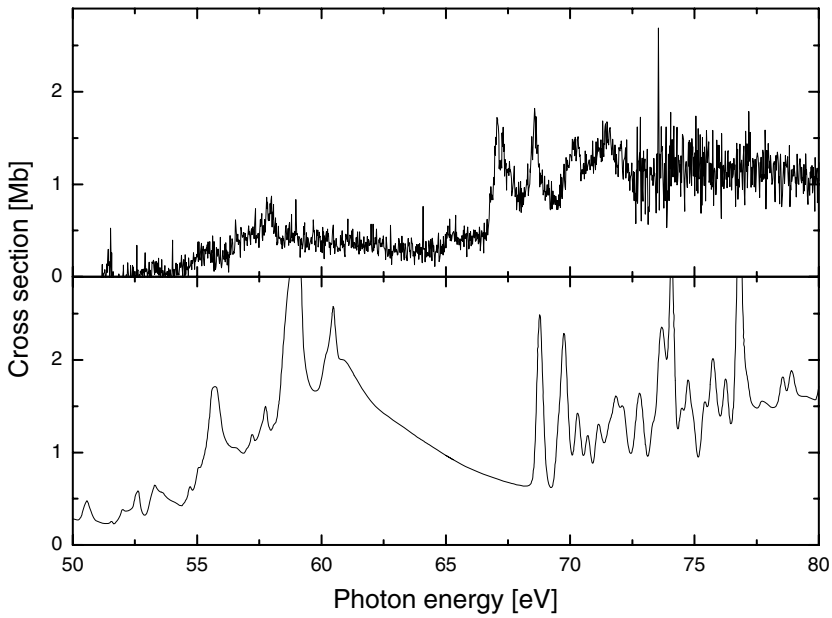

Figure 5. Similar to figure 4 but showing the $Fe^{+} \rightarrow Fe^{3+}$ double-photoionization cross section.

is a group of intense, broad and overlapping resonance structures embedded in the $3d^6 4s\epsilon l$ continua.

The $Fe^{+} \rightarrow Fe^{3+}$ double-photoionization cross section, see figure 5, is characterized by a slow onset that begins near 52 eV, a step-like increase at 66.9 eV, several broad structures in the region below 75 eV and an almost constant cross section with a magnitude of $\sim$1.3 Mb for photon energies ranging from 75 eV to the maximum energy employed in the experiments, 180 eV. We expect that the edge at 66.9 eV is related to the lowest of the Fe^{2+} $3p^{-1}$ thresholds and that the main mechanism for Fe^{3+} production above this energy is photoionization of the Fe^{+} ions into the Fe^{2+} $3p^{-1} + e_{photo}$ continua followed by rapid Auger decay of the Fe^{2+} ions to $Fe^{3+} + e_{Auger}$. On the other hand, the spectral structures could also be related to photoexcitation to excited states of Fe^{+} with configurations of the type $3p^{-1}3d^x4s$ which may decay to Fe^{3+} by double (cascade?) autoionization. The strong perturbation of the double-ionization cross section near 67 eV shows that the interaction between direct and indirect double photoionization is strong.

To our knowledge, there has only been reported a single investigation of the spectral structure in the $3p^{-1}$ region of Fe^{+}, the recent *R*-matrix calculation by Berrington and Ballance (2001). In figure 4, the experimental data for single photoionization have been compared with the calculated data, with the result that the observed overall structure of the cross section is reproduced quite well. For both data sets we notice two broad, asymmetric structures and some sharper but weaker peaks (only one peak in the calculation) approximately in the middle of the resonance region. The details of the cross section, on the other hand, are not reproduced correctly—the calculation predicts a maximum value of the cross section that is too large and the entire resonance structure is too broad and positioned at too high an energy. Furthermore, additional structures are predicted between 68 and 78 eV whereas the experimental spectrum is smooth in that region. The main purpose of the study of Berrington and Ballance (2001) was to calculate the double- rather than the single-photoionization cross section. For the double-

ionization cross section the discrepancies with respect to the experimental data are, however, much more pronounced than for the single-ionization cross section, even though the calculated cross section still exhibits some resemblance to the experimental one, see figure 5.

It is interesting to compare the spectra for neutral Fe($3d^6 4s^2\ ^5D$) and Fe^+ ($3d^6 4s\ ^6D$) in the $3p \rightarrow 3d$ region. For single ionization, the photo-ion yield data by Feist *et al* (1996) for neutral Fe and the present absolute photoionization cross-section data exhibit a strong resemblance, the main difference being the lack of the $3p \rightarrow 4s$ resonances in the spectrum for neutral Fe. On the other hand, the double-ionization spectra are very different below the respective $3p^{-1}$ limits. For neutral Fe, the double-ionization cross section possesses a structure almost identical to that of the single-ionization cross section, and the ratio between the double- and single-ionization yields exhibits a nearly constant value of ∼20% (Feist *et al* 1996). For Fe^+ double ionization contributes only about 2% of the single-ionization cross section in the corresponding region and the double- and single-ionization spectra exhibit different spectral structures; this may indicate that the channels responsible for the double ionization are different from the channels dominating the single-ionization cross section. In both cases, the double-ionization cross section increases abruptly at the $3p^{-1}$ ionization limits, and above these limits the double-ionization (continuum) cross sections have nearly constant values.

Berrington and Ballance (2001) made similar observations from their calculations: the single-ionization spectra were noticed to be very similar and the double-ionization spectra different. It should be noted, however, that for both species the calculated data by Ballance and Berrington only exhibit a relatively weak resemblance to the experimental ones (compare the spectra published by Feist *et al* (1996) and Berrington and Ballance, respectively, for the case of neutral Fe, and see figure 5 for Fe^+).

3.3. The magnitude of the absolute cross section

The magnitude of the photoionization cross section is important for the modelling of different physical systems, and it is therefore reasonable to compare the present experimental data with the different data sets available for such modellings. The threshold region has already been discussed above and will not be considered further here. As pointed out above, the present experimental data are not accurate with respect to the magnitude of the photoionization cross section for photon energies below ∼25 eV.

It is evident from the experimental data that excitation of the 3p inner-shell electrons strongly affects the photoionization cross section. However, the calculations in the Opacity Project were performed using a low-energy approximation, and inner-shell photoionization processes were generally not considered. Thus, the calculation by Nahar and Pradhan (1994) for Fe^+ was only performed using the *R*-matrix method in the low-energy region whereas the high-energy tail (in the present case, the cross section for $h\nu \geqslant 30$ eV) was given by some kind of exponentially decreasing function. The magnitude and shape of this function deviate strongly from the experimental photoionization cross section, the calculated cross section being about ten times smaller than the experimental one at 80 eV for example. From an atomic-physics point of view this deviation is not surprising, but the fact that calculated data are provided for energies outside the region of validity of the theoretical approximation may be a source of confusion and should be avoided.

In contrast to the calculations in the Opacity Project, the more recent *R*-matrix calculations by Berrington and Ballance ((2001), see figures 4 and 5) describe the photoionization cross section in the 3p-excitation region. It has already been noted in the previous section that the $3p \rightarrow 3d$ giant resonance was predicted to be positioned at too high energy and with a too large maximum cross section. Furthermore, the integrated cross section (the total oscillator strength)

in the 50–80 eV region is about 50% larger for the calculated single-ionization cross section than for the measured one, with the corresponding number being 90% for double ionization.

For modelling of e.g. astrophysical systems, the detailed spectral structure is not always the central issue, and often the average cross section (with the averaging performed over an appropriate energy region) is more important. As a consequence, analytical model functions or averaged cross sections have been provided and are often used. Such data have the advantage that much less computer power is required to carry out a certain modelling, but of course no information concerning the detailed spectral structure will be included. Examples of such cross-section data are the Hartree–Slater calculations by Reilman and Manson (1978, 1979), the model functions provided by Verner *et al* (1993, 1996), Verner and Yakovlev (1995) and the resonance averaged photoionization (RAP) cross sections provided by Bautista *et al* (1998) respectively. The RAP data are obtained by averaging the data obtained in the Opacity Project and will not be considered further here.

Reilman and Manson (1978) have calculated the inner-shell as well as valence-shell photoionization cross sections (per electron) for Fe^+ and other Fe ions using the Hartree–Slater central-potential model. Their data are shown in figure 1. We have included their cross-section data for excitation of 4s, 3d, 3p and 3s electrons, although it is possible that photoionization of the 3s electrons may result in triple ionization (Fe^{4+} ions were not detected in the present experiment). However, the question of including the 3s photoionization or not is only of minor importance for the value of the total cross section in the energy range considered in the present paper. It can be observed that the high-energy tail of the experimental cross section is reproduced with good accuracy by the calculation. For lower photon energies, $h\nu \leqslant 70$, strong deviations are noticed. Some of these can be attributed to the 'perturbation' of the experimental cross section by the autoionizing resonances and such effects were not included in the relatively simple theoretical model, but also the continuum cross section in the 30–50 eV region is incorrect.

The total photoionization cross section obtained using the model functions for the subshell cross sections of Fe^+ provided by Verner *et al* (1993) is essentially equal to the cross section provided by Reilman and Manson. This is not surprising since the two data sets are based on similar central-field approximations; Reilman and Manson performed Hartree–Fock–Slater calculations whereas Verner *et al* obtained their model functions by fitting to data obtained using Hartree–Dirac–Slater calculations. The data by Verner *et al* are therefore not shown here, and instead we refer to the discussion in the previous paragraph. The data reported by Verner *et al* (1996) are shown in figure 1, but for this data set also the agreement with experiment is poor for low energies.

In relation to the discussion in the previous section, it should be mentioned that the calculated magnitudes (Reilman and Manson 1978, Verner *et al* 1993) of subshell photoionization cross sections for 3s and 3p or 3d and 4s photoionization agree (for photon energies larger than $\sim$100 eV) with the measured double- and single-ionization cross sections respectively. This shows that double ionization is mainly due to photoionization of the 3s and 3p inner-shell electrons followed by Auger decay as postulated, whereas single ionization is due to photoionization of the 3d (and to a lesser extent also the 4s) electrons; the latter is strongly perturbed by the interaction with 3p photoexcitation in the 50–70 eV region, however.

4. Conclusion

We have measured absolute cross-section data for single and double photoionization of Fe^+ ions from 15.8 to 180 eV using the merged-beam technique. *R*-matrix calculations (Nahar and Pradhan 1994, Berrington 2002a) reproduce the main features of the low-energy part

of the spectrum, yet significant discrepancies are observed. Furthermore, the importance of using a sufficiently fine energy grid in the calculations was discussed and should be emphasized. The calculation by Berrington and Ballance (2001, *R*-matrix) reproduces the general features of the 3p-excitation region correctly in the case of single ionization but does not perform so well for double ionization. Significant deviations are observed between the present experimental data and Hartree–Fock–Slater calculations (Reilman and Manson 1978) and Hartree–Dirac–Slater calculations (Verner *et al* 1993, 1996) for low energies, whereas these calculations reproduce the high-energy tail of the cross section with good accuracy. There exists no calculation which reproduces the present experimental data correctly in the entire energy region investigated here (15.8–180 eV). As input data for modelling, we recommend the use of the recent calculation by Berrington (2002a) or the calculation by Nahar and Pradhan ((1994), recalculated with a finer energy grid) for the low-energy region, $h\nu \leqslant 25$ eV, and the present experimental data for the region 25–180 eV; the latter are available at http://www.ifa.au.dk/amo/atomphys/atomphys.htm.

Acknowledgments

The ion–photon project is part of the research programme for the Aarhus Center for Atomic Physics (ACAP), funded by the Danish National Research Foundation. During the preparation of the manuscript we have had valuable discussions with Sultana Nahar and Anil Pradhan (Ohio State University), Michael Martins (Hamburg University), Jørgen Hansen (University of Amsterdam) and Keith Berrington (Sheffield Hallam University). We thank Sultana Nahar for performing the fine energy-grid calculations, Keith Berrington for providing us with data prior to publication and the staff of the Institute for Storage Ring Facilities (ISA) at the University of Aarhus for their expert assistance throughout the period of the project.

References

Almen O and Nielsen K 1957 *Nucl. Instrum. Methods* **1** 302
Bautista M A, Romano P and Pradhan A K 1998 *Astrophys. J. Suppl.* **118** 259
Berrington K 2002a *J. Phys. B: At. Mol. Opt. Phys.* in preparation
Berrington K 2002b private communication
Berrington K A and Ballance B 2001 *J. Phys. B: At. Mol. Opt. Phys.* **34** L383
Covington A M *et al* 2001 *Phys. Rev. Lett.* **87** 243002
Feist H, Feldt M, Gerth Ch, Martins M, Sladeczek P and Zimmermann P 1996 *Phys. Rev.* A **53** 760
Hansen H *et al* 1977 *J. Phys. B: At. Mol. Phys.* **10** 37
Kjeldsen H, Folkmann F, Hansen J E, Knudsen H, Rasmussen M S, West J B and Andersen T 1999a *Astrophys. J.* **524** L146
Kjeldsen H, Folkmann F, Knudsen H, Rasmussen M S, West J B and Andersen T 1999b *J. Phys. B: At. Mol. Opt. Phys.* **32** 4457
Kjeldsen H, Folkmann F, Hansen J E, Knudsen H, Rasmussen M S, West J B and Andersen T 2001 *Astrophys. J. Suppl.* **135** 53 193
Kjeldsen H, Kristensen B, Brooks R L, Folkmann F, Knudsen H and Andersen T 2002a *Astrophys. J. Suppl.* **138** 219
Kjeldsen H, Andersen P, Folkman F, Hansen J E, Kitajima M and Andersen T 2002b *J. Phys. B: At. Mol. Opt. Phys.* **35** 2845
Kjeldsen H, Folkman F, Innocenti F, Zuin L and Hansen J E 2002c *J. Phys. B: At. Mol. Opt. Phys.* **35** L375
Kjeldsen H, West J B, Folkmann F, Knudsen H and Andersen T 2000 *J. Phys. B: At. Mol. Opt. Phys.* **33** 1403
Kristensen B, Andersen T, Folkmann F, Kjeldsen H and West J B 2002 *Phys. Rev.* A **65** 022707
Li Z S, Lundberg H, Berzinsh U, Johansson S and Svanberg S 2000 *J. Phys. B: At. Mol. Opt. Phys.* **33** 5593
Lombardi G G, Smith P L and Parkinson W H 1978 *Phys. Rev.* A **18** 2131
Lyon I C, Peart B, West J B and Dolder K 1986 *J. Phys. B: At. Mol. Phys.* **19** 4137
Martins M 2001 private communication
Müller *et al* 2002 *J. Phys. B: At. Mol. Opt. Phys.* **35** L137

Nahar S N 1996 *Phys. Rev.* A **53** 2417
Nahar S N 1997 *Phys. Rev.* A **55** 1980
Nahar S N 2002 private communication
Nahar S N and Pradhan A K 1994 *J. Phys. B: At. Mol. Opt. Phys.* **27** 429
NIST 2002 *The NIST Atomic Spectra Database, version 2.0*, webpage http://physics.nist.gov/
Pradhan A K 2002 private communication
Reilman R F and Manson S T 1978 *Phys. Rev.* A **18** 2124
Reilman R F and Manson S T 1979 *Astrophys. J. Suppl.* **40** 815
Rostobar D, Derkartch A, Hartman H, Johansson S, Lundberg H, Mannervik S, Norlin L-O, Royen P and Schmitt A 2001 *Phys. Rev. Lett.* **86** 1466
Sawey P M J and Berrington K A 1992 *J. Phys. B: At. Mol. Opt. Phys.* **25** 1451
Seaton M J 1987 *J. Phys. B: At. Mol. Phys.* **20** 6409
Sonntag B and Zimmermann P 1992 *Rep. Prog. Phys.* **55** 911
Sugar J and Corliss C 1985 *J. Phys. Chem. Ref. Data* **14**
The Opacity Project Team 1995 *The Opacity Project* vol 1 (Bristol: Institute of Physics Publishing)
Verner D A, Ferland G J and Korista K T 1996 *Astrophys. J.* **465** 487
Verner D A and Yakovlev D G 1995 *Astrophys. J. Suppl.* **109** 125
Verner D A, Yakovlev D G, Band I M and Trzhaskovskaya M B 1993 *At. Nucl. Data Tables* **55**
West J B 2001 *J. Phys. B: At. Mol. Opt. Phys.* **34** R45
West J B, Andersen T, Brooks R L, Folkmann F, Kjeldsen H and Knudsen H 2001 *Phys. Rev.* A **63** 052719